International Journal of Heat and Mass Transfer 52 (2009) 2370–2378

Contents lists available at ScienceDirect

International Journal of Heat and Mass Transfer

journal homepage: www.elsevier.com/locate/ijhmt

A review on reduction method for heat and mass transfer characteristics of fin-and-tube heat exchangers under dehumidifying conditions

Worachest Pirompugd [a], Chi-Chuan Wang [b], Somchai Wongwises [c,*]

[a] Department of Mechanical Engineering, Faculty of Engineering, Burapha University, Saensook, Muang, Chonburi 20131, Thailand
[b] Energy and Environment Research Lab., Industrial Technology Research Institute, Hsinchu 310, Taiwan, ROC
[c] Fluid Mechanics, Thermal Engineering and Multiphase Flow Research Lab. (FUTURE), Department of Mechanical Engineering, King Mongkut's University of Technology Thonburi, Bangmod, Bangkok 10140, Thailand

ARTICLE INFO

Article history:
Received 13 March 2008
Received in revised form 23 October 2008
Available online 30 December 2008

Keywords:
Dehumidifying condition
Fin-and-tube heat exchanger
Heat mass and momentum transfer
Reduction method

ABSTRACT

This paper presents a review of data reduction method for heat and mass transfer characteristics of fin-and-tube heat exchangers with dehumidification. There are many reduction methods for fin-and-tube heat exchangers under dehumidifying conditions. The data reduction methods being reviewed includes the original Threlkeld method, direct method, the equivalent dry-bulb method, tube by tube method, the fully wet and fully dry tiny circular fin method, and the finite circular fin method. Among these methods, the original Threlkeld method, direct method, the equivalent dry-bulb method are lumped method while others can divide the fin-and-tube heat exchangers into small segments for more accuracy in handling the surfaces to be fully dry, fully wet, or partially wet. In addition, the mass transfer characteristics can be obtained from the modified process line equation incorporated with the preceding methods. It should be noted that the conventional assumption of constant ratio ($h_{c,o}/h_{d,o}C_{p,a} \approx$ constant) is actually incorrect. This present paper can be used as the first guideline for the researcher for reducing the experimental data for fin-and-tube heat exchangers under dehumidifying conditions.

1. Introduction

Fin-and-tube heat exchangers are widely used in applications of HVAC&R (heating, ventilating, air-conditioning, and refrigeration) systems. They include a group of fins arranged parallel to themselves at a constant spacing. The configuration of fins can be either continuous (plain or wavy) or interrupted (louver, slit or the like). One or more tubes which take the forms of either circular, flat, or oval configuration are arranged perpendicularly to the direction of air flow. The fin-and-tube heat exchangers can be applicable to condensers and evaporators. In evaporators, which typically use aluminum fins with the surface temperature generally being below the dew point temperature result in simultaneous heat and mass transfer outside tube and fin surfaces. In practice, the fin surfaces may be fully wet or partially wet depending on the local difference between fin surface temperature and dew point temperature. Many researchers presented the mathematical model for predicting the heat and mass transfer characteristics of moist air for fin-and-tube heat exchanger. It is therefore the objective of this review article to present relevant reduction method concerning the heat, mass, and momentum transfer characteristic of fin-and-tube heat exchangers.

2. Experimental apparatus

Many published literatures had experimentally investigated the heat and mass transfer characteristics of the fin-and-tube heat exchanger under dehumidification. A typical schematic diagram of the experimental air circuit assembly is shown in Fig. 1. It consists of a closed-loop wind tunnel in which air is circulated by a variable speed centrifugal fan. The dry-bulb and wet-bulb temperatures of the inlet-air are controlled by an air-ventilator. The air flow-rate measurement station is an outlet chamber set up with multiple nozzles. It is recommended that the setup is constructed following the ASHRAE 41.2 standard [1] and applied a differential pressure transducer is used to measure the pressure difference across the nozzles. It is also recommended that the air temperatures at the inlet and exit zones across the sample heat exchangers are measured by two psychrometric boxes based on the ASHRAE 41.1 standard [2]. The energy imbalance should satisfy the ASHRAE [3] requirements (namely, the energy balance condition, $\left|\dot{Q}_r - \dot{Q}_a\right|/\dot{Q}_{avg}$, is less than 0.05, where $\dot{Q}_r$ is the water side heat transfer rate and $\dot{Q}_a$ is the air-side heat transfer rate) are considered in the final analysis.

* Corresponding author. Tel.: +66 2 470 9115; fax: +66 2 470 9111.
E-mail address: somchai.won@kmutt.ac.th (S. Wongwises).

0017-9310/$ - see front matter © 2008 Elsevier Ltd. All rights reserved.
doi:10.1016/j.ijheatmasstransfer.2008.10.019

Nomenclature

$A_{c,min}$	minimum moist air flow area, m^2
A_f	surface area of the fin, m^2
$A_{p,j}$	inside surface area of the tube, m^2
$A_{p,o}$	outside surface area of the tube, m^2
A_o	total air-side surface area that is the summation of A_f and $A_{p,o}$, m^2
b'_p	slope of the saturated moist air enthalpy curved between the mean inside and outside tube surface temperatures, J kg^{-1} K^{-1}
b'_r	slope of the saturated moist air enthalpy curved between the mean water temperature and the mean inside tube surface temperature, J kg^{-1} K^{-1}
$b'_{w,f}$	slope of the saturated moist air enthalpy curved at the mean water film temperature of the fin surface, J kg^{-1} K^{-1}
$b'_{w,p}$	slope of the saturated moist air enthalpy curved at the mean water film temperature of the outside tube surface, J kg^{-1} K^{-1}
c	concentration, mol m^{-3}
D	mass diffusivity, m^2 s^{-1}
$C_{p,a}$	moist air specific heat at the constant pressure, J kg^{-1} K^{-1}
D_c	collar diameter, m
D_i	inside tube diameter, m
F	correction factor
f	moist air-side friction factor
f_r	water side friction factor
$G_{c,min}$	moist air mass velocity based on the minimum moist air flow area, kg m^{-2} s^{-1}
$h_{c,o}$	moist air-side convection heat transfer coefficient, W m^{-2} K^{-1}
$h_{d,o}$	moist air-side convection mass transfer coefficient, kg m^{-2} s^{-1}
h_r	water side convection heat transfer coefficient, W m^{-2} K^{-1}
I_0	modified Bessel function solution of the first kind, order 0.
I_1	modified Bessel function solution of the first kind, order 1.
i_a	moist air enthalpy, J kg^{-1}
$i_{a,in}$	inlet moist air enthalpy, J kg^{-1}
$i_{a,m}$	mean moist air enthalpy, J kg^{-1}
$i_{a,out}$	outlet moist air enthalpy, J kg^{-1}
i_{fg}	enthalpy of vaporization of water, J kg^{-1}
i_g	saturated water vapor enthalpy, J kg^{-1}
$i_{s,r,in}$	saturated air enthalpy at the inlet water temperature, J kg^{-1}
$i_{s,r,m}$	mean saturated moist air enthalpy at the mean water temperature for the counter flow configuration, J kg^{-1}
$i_{s,r,out}$	saturated air enthalpy at the outlet-water temperature, J kg^{-1}
$i_{s,p,o,m}$	mean saturated air enthalpy at the mean outside tube wall temperature, J kg^{-1}
$i_{s,wf,m}$	mean saturated air enthalpy at the mean water film temperature of the fin surface, J kg^{-1}
j_h	Colburn heat transfer group or Chilton-Colburn j-factor for the heat transfer
j_m	Colburn mass transfer group or Chilton-Colburn j-factor for the mass transfer
K_0	modified Bessel function solution of the second kind, order 0
K_1	modified Bessel function solution of the second kind, order 1
K_i	entrance loss coefficient
K_e	exit loss coefficient
k_f	thermal conductivity of the fin, W m^{-1} K^{-1}
k_m	mass transfer coefficient (based on c), m s^{-1}
k_p	thermal conductivity of the tube, W m^{-1} K^{-1}
k_r	thermal conductivity of the water, W m^{-1} K^{-1}
k_w	thermal conductivity of the water film, W m^{-1} K^{-1}
L	characteristics length, m
L_p	tube length, m
N	number of tube row
Nu	Nusselt number
P_1	longitudinal tube pitch, m
Pr	Prandtl number
Pr_r	water side Prandtl number
P_t	transverse tube pitch, m
$\dot{Q}_a$	moist air-side heat transfer rate, W
$\dot{Q}_{avg}$	average heat transfer rate between the moist air and water sides, W
$\dot{Q}_{dry}$	heat transfer rate for fully dry segment, W
$\dot{Q}_{dry,conv,\max}$	maximum heat transfer rate for dry portion in partially wet segment, W
$\dot{Q}_r$	water side heat transfer rate, W
$\dot{Q}_{wet}$	heat transfer rate for a fully wet segment, W
$\dot{Q}_{wet,conv,\max}$	maximum heat transfer rate for wet portion in partially wet segment, W
$\dot{Q}'_{wet,conv,\max}$	maximum heat transfer rate for partially wet segment, W
R	ratio of the convection heat transfer characteristic to the convection mass transfer characteristic for the simultaneous convection heat and mass transfer
Re_{Dc}	moist air-side Reynolds number based on the collar diameter
Re_{Di}	water side Reynolds number
r_i	inside fin radius for the equivalent circular area method that equal to the outside tube (include collar) radius, m
r_o	outside fin radius for the equivalent circular area method, m
r^*	distance from the center of the tube to the interface, m
Sc	Schmidt number
Sh	Sherwood number
T_a	moist air temperature, K
T_a^e	equivalent dry-bulb temperature, K
$T_{a,in}$	inlet moist air temperature, K
$T_{a,m}$	mean moist air temperature for the counter flow configuration, K
$T_{a,out}$	outlet moist air temperature, K
T_{dp}	dew point temperature of the moist air, K
$T_{f,b}$	fin base temperature, K
$T_{f,t}$	fin tip temperature, K
$T_{f,m}$	mean fin temperature, K
$T_{p,o}$	outside tube surface temperature, K
$T_{p,o,m}$	mean outside tube surface temperature for the counter flow configuration, K
T_r	water temperature, K
$T_{r,in}$	inlet water temperature, K
$T_{r,m}$	mean water temperature for the counter flow configuration, K
$T_{r,out}$	outlet-water temperature, K
t	fin thickness, m
U_i	inside heat transfer coefficient, based on temperature difference, W m^{-2} T^{-1}
$U_{o,d}$	overall heat transfer coefficient for fully dry surface condition, based on temperature difference, W m^{-2} T^{-1}
$U_{o,w}$	overall heat transfer coefficient for fully wet surface condition, based on enthalpy difference kg m^{-2} s^{-1}
V_r	water velocity, m s^{-1}
W_a	moist air humidity ratio

$W_{a,m}$	mean moist air humidity ratio
$W_{s,p,o}$	saturated air humidity ratio at the outside tube temperature
$W_{s,p,o,m}$	mean saturated air humidity ratio at the mean outside tube temperature
$W_{s,w,f,m}$	mean saturated air humidity ratio at the mean water film temperature at the fin surface
y_w	thickness of the water film, m
ρ_i	inlet moist air density, kg m^{-3}
ρ_m	mean moist air density, kg m^{-3}
ρ_o	outlet moist air density, kg m^{-3}
ρ_r	water density, kg m^{-3}
μ_r	viscosity of water, kg m^{-1} s^{-1}
σ	ratio of minimum flow area to frontal area
$\eta_{f,dry}$	fully dry fin efficiency
$\eta_{f,part}$	partially wet fin efficiency
$\eta'_{f,part}$	effectively partially wet fin efficiency
$\eta_{f,wet}$	fully wet fin efficiency
θ_{dry,r^*}	air temperature difference at r^*, K
θ_{wet,r_i}	air enthalpy difference at r_i, kJ kg^{-1}
Δi_m	logarithmic mean enthalpy difference across the heat exchanger for the counter flow double-pipe configuration with the hot and cold fluid enthalpies, kJ kg^{-1}
ΔP	pressure difference, N m^{-2}
ΔT_m	logarithmic mean temperature difference across the heat exchanger for the counter flow double-pipe configuration with the hot and cold fluid temperatures, K

3. Mathematical model for heat transfer

3.1. Enthalpy difference method

In 1970, Threlkeld [4] presented the mathematical model for calculating the heat transfer of fin-and-tube heat exchanger. This method is commonly used for designing (ASHRAE [3]). In many published literatures, the authors used this method for the data reduction (e.g. Jacobi and Goldschimildt [5]; Wang et al. [6]; Corberan and Melon [7]; Wang et al. [8,9]; Kim and Bullard [10]; Wang et al. [11], Kim et al. [12,13]). This model is based on the enthalpy potential applicable to a process of sensible cooling and dehumidifying. The heat transfer rate can be calculated from the product of overall heat transfer coefficient, surface area, logarithmic mean enthalpy difference and correction factor as shown in Eq. (1)

$$\dot{Q}_{wet} = U_{o,w} A_o \Delta i_m F, \tag{1}$$

where Δi is the mean enthalpy difference for a counter flow coil,

$$\Delta i_m = i_{a,m} - i_{s,r,m}. \tag{2}$$

According to Bump [14] and Myers [15], for the counter flow configuration, the mean enthalpy is

$$i_{a,m} = i_{a,in} + \frac{i_{a,in} - i_{a,out}}{\ln\left(\frac{i_{a,in} - i_{s,r,out}}{i_{a,out} - i_{s,r,in}}\right)} - \frac{(i_{a,in} - i_{a,out})(i_{a,in} - i_{s,r,out})}{(i_{a,in} - i_{s,r,out}) - (i_{a,out} - i_{s,r,in})}, \tag{3}$$

$$i_{s,r,m} = i_{s,r,out} + \frac{i_{s,r,out} - i_{s,r,in}}{\ln\left(\frac{i_{a,in} - i_{s,r,out}}{i_{a,out} - i_{s,r,in}}\right)} - \frac{(i_{s,r,out} - i_{s,r,in})(i_{a,in} - i_{s,r,out})}{(i_{a,in} - i_{s,r,out}) - (i_{a,out} - i_{s,r,in})}. \tag{4}$$

Upon adopting the enthalpy-based reduction method, the overall resistance is related to the individual heat transfer resistance as follows:

$$\frac{1}{U_{o,w}} = \frac{b'_r A_o}{h_r A_{p,i}} + \frac{b'_p A_o \ln\left(\frac{D_c}{D_i}\right)}{2\pi k_p L_p} + \frac{1}{h_{o,w}\left(\frac{A_{p,o}}{b'_{w,p} A_o} + \frac{A_f \eta_{f,wet}}{b'_{w,f} A_o}\right)}, \tag{5}$$

where

$$h_{o,w} = \frac{1}{\frac{C_{p,a}}{b'_{w,f} h_{c,o}} + \frac{y_w}{k_w}}, \tag{6}$$

y_w in Eq. (6) is the thickness of the water film. A constant of 0.005 inch was proposed by Myers [15]. The water side heat transfer coefficient, h_r is evaluated from the Gnielinski correlation [16],

$$h_r = \frac{(f_r/2)(Re_{D_i} - 1000)Pr_r}{1.07 + 12.7\sqrt{f_r/2}(Pr_r^{2/3} - 1)} \cdot \frac{k_r}{D_i} \tag{7}$$

and the friction factor, f_r is

$$f_r = \frac{1}{(1.58 \ln Re_{D_i} - 3.28)^2}. \tag{8}$$

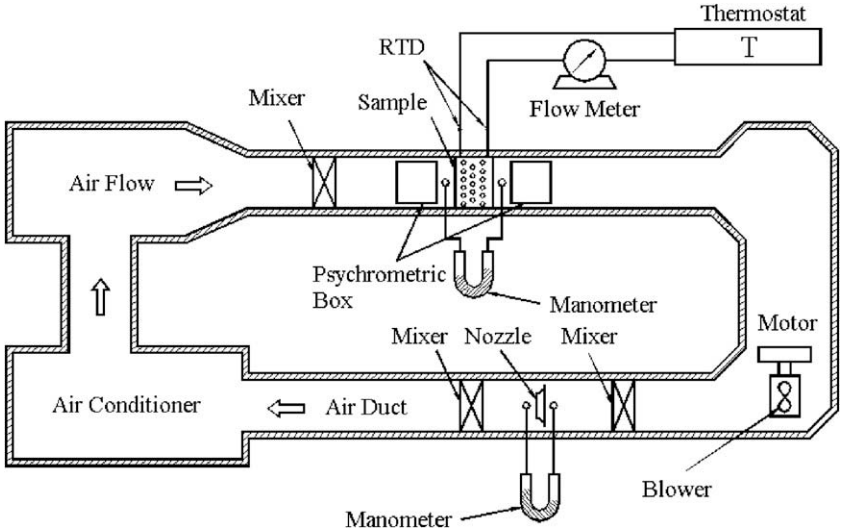

Fig. 1. Schematic diagram of experimental apparatus.

The Reynolds number used in Eqs. (7) and (8) is determined from $Re_{D_i} = \rho_r V_r D_i/\mu_r$. It is based on the inside diameter of the tube.

The wet fin efficiency was presented from previous publication. McQuiston [17] developed the wet fin efficiency for a straight fin (Fig. 2) based on the temperature difference. McQuiston and Parker [18] extended the analysis to circular fins (Fig. 2) using the approximation proposed by Schmidt [19]. This analysis is based on the temperature difference. The wet fin efficiency is given as

$$\eta_{f,wet} = \frac{\tanh M_T r_i \theta}{M_T r_i \theta}, \tag{9}$$

where

$$M_T = \sqrt{\frac{2h_{c,o}}{k_f t}\left(1 + \frac{Ci_{fg}}{C_{p,a}}\right)}, \tag{10}$$

$$\theta = \left(\frac{r_o}{r_i} - 1\right)\left[1 + 0.35\ln\left(\frac{r_o}{r_i}\right)\right], \tag{11}$$

and the constant C in Eq. (10) is given by

$$C = \frac{W_a - W_{s,p,o}}{T_a - T_{p,o}}. \tag{12}$$

Threlkeld [4] presented the wet fin efficiency for a straight fin based on the enthalpy difference. The wet fin efficiency can be applied to the circular fins using the same analysis proposed by McQuiston and Parker [18].

$$\eta_{f,wet} = \frac{\tanh M'_T r_i \theta}{M'_T r_i \theta}, \tag{13}$$

where

$$M'_T = \sqrt{\frac{2h_{o,w}}{k_f t}}. \tag{14}$$

Hong and Webb [20] derived the analytical formulation of circular fin under fully wet surface condition. This analytical formulation is based on the temperature difference.

$$\eta_{f,wet} = \frac{2r_i}{M_T(r_o^2 - r_i^2)}\left[\frac{K_1(M_T r_i)I_1(M_T r_o) - K_1(M_T r_o)I_1(M_T r_i)}{K_1(M_T r_o)I_0(M_T r_i) + K_0(M_T r_i)I_1(M_T r_o)}\right] \tag{15}$$

Wang et al. [6] derived the wet fin efficiency developed from Threlkeld [4] and Hong and Webb [20]. The derivation is based on the enthalpy difference.

$$\eta_{f,wet} = \frac{2r_i}{M'_T(r_o^2 - r_i^2)}\left[\frac{K_1(M'_T r_i)I_1(M'_T r_o) - K_1(M'_T r_o)I_1(M'_T r_i)}{K_1(M'_T r_o)I_0(M'_T r_i) + K_0(M'_T r_i)I_1(M'_T r_o)}\right] \tag{16}$$

The evaluation of plate fin efficiency (Fig. 2) is calculated by the equivalent circular area method as shown in Fig. 3.

Note that Eq. (5) introduces the ratio of enthalpy to temperature like $b'_r, b'_p, b'_{w,p}$ and $b'_{w,f}$. However, typical lumped approach

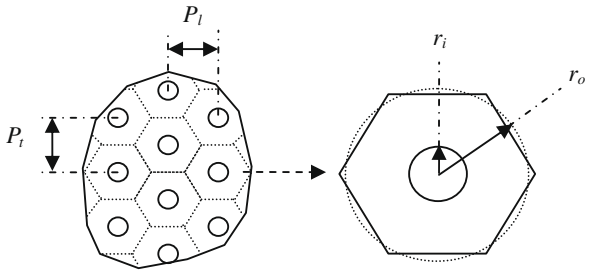

Fig. 3. Equivalent circular area method.

presumes these ratios are constant as aforementioned by many published literatures. This may be applicable for a refrigeration-based heat exchanger where temperature is considered unchanged. Unfortunately, most of the experiments are performed using water as the chilling medium, thereby leading a detectable change of water temperature. As a consequence, the reduction method using the lumped approach may overlook the influence of variables like $b'_r, b'_p, b'_{w,p}, b'_{w,f}$ or even the wet efficiency $\eta_{f,wet}$.

Pirompugd et al. [21,22] presented so-called "tube-by-tube method (TTM)" reduction method. The TTM stems from the Threlkeld's method. Through the TTM, the fin-and-tube heat exchanger is further divided into many small segments equaling to the multiplication of the number of tube row and the number of tube pass per row and number of fin as shown in Fig. 4. Upon this approach, the water temperature in each segment is almost constant. The equivalent circular area method for approximation to the circular fin is adopted and is also shown in Fig. 3. The Threlkeld's method must be applied to all segments and the all equation must be solved simultaneously. The detailed calculation procedure can be found in Pirompugd et al. [21,22].

However, the Threlkeld's method and the TTM are based on the assumption of all fin and outside tube surfaces are assumed to be in fully wet surface condition. However, some outside surface may be dry if the corresponding surface temperature is above dew point temperature of the moist air. To resolve this concern, Pirompugd et al. [23,24] developed the mathematical model for the partially wet surface condition. The new model namely "fully wet and fully dry tiny circular fin method (WDFM)" is made by dividing the fin-and-tube heat exchanger into many tiny segment similar to that of the TTM. For the WDFM, the data reduction method for every segments depends on its corresponding temperature difference of surface and dew point temperature as shown in Fig. 5. If the dew point temperature of moist air is higher than the outside tube surface temperature, the fully wet surface condition prevails. By contrast, when the dew point temperature of moist is lower than the outside tube surface temperature, the surface is regarded as fully dry. The details for calculation for the fully wet segment are virtually the same as that of the TTM while the

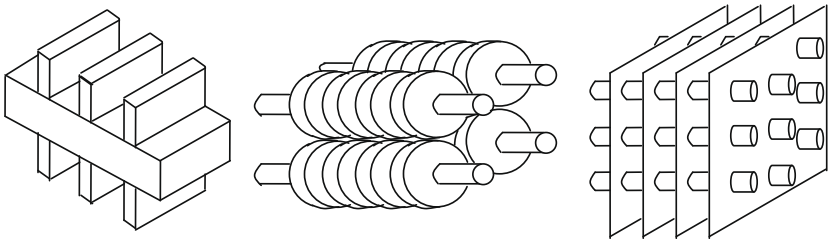

(2.1) Straight Fin (2.2) Circular Fin (2.3) Continuous plate Fin

Fig. 2. Type of fin configuration.

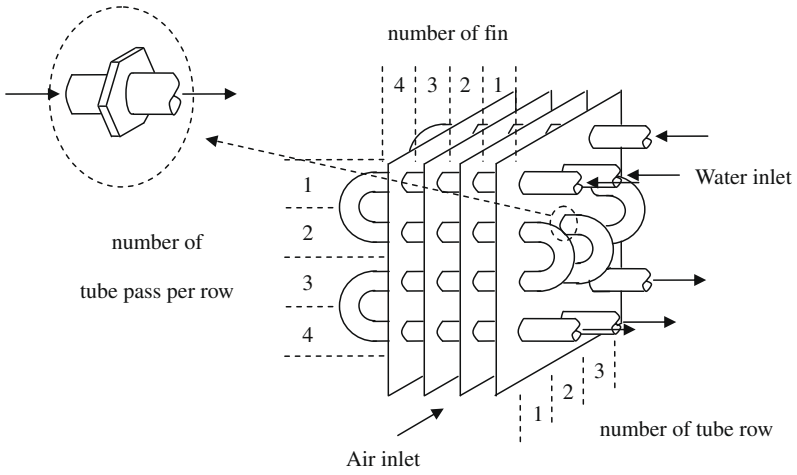

Fig. 4. Schematic of the dividing of the fin-and-tube heat exchanger into many tiny segments.

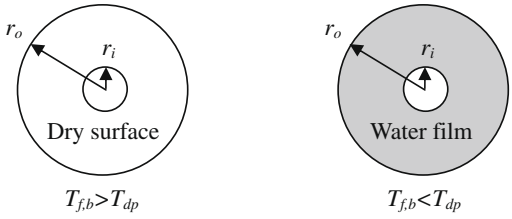

(5.1) Fully dry condition (5.2) Fully wet condition

Fig. 5. Circular fin in fully dry and fully wet surface conditions.

fully dry segments incorporates the rate equation based on the temperature difference (Eq. (18)).

$$\dot{Q}_{dry} = U_{o,d} A_o \Delta T_m F \tag{17}$$

The term of ΔT_m is the logarithm temperature difference

$$\Delta T_m = T_{a,m} - T_{r,m} \tag{18}$$

According to Bump [14], for the counter flow configuration, the mean temperature difference is

$$T_{a,m} = T_{a,in} + \frac{T_{a,in} - T_{a,out}}{\ln\left(\frac{T_{a,in} - T_{r,out}}{T_{a,out} - T_{r,in}}\right)} - \frac{(T_{a,in} - T_{a,out})(T_{a,in} - T_{r,out})}{(T_{a,in} - T_{r,out}) - (T_{a,out} - T_{r,in})} \tag{19}$$

$$T_{r,m} = T_{r,out} + \frac{T_{r,out} - T_{r,in}}{\ln\left(\frac{T_{a,in} - T_{r,out}}{T_{a,out} - T_{r,in}}\right)} - \frac{(T_{r,out} - T_{r,in})(T_{a,in} - T_{r,out})}{(T_{a,in} - T_{r,out}) - (T_{a,out} - T_{r,in})} \tag{20}$$

For all fully dry segments, the temperature based overall heat transfer coefficient is as follows:

$$\frac{1}{U_{o,d}} = \frac{A_o}{h_r A_{p,i}} + \frac{A_o \ln\left(\frac{D_c}{D_i}\right)}{2\pi k_p L_p} + \frac{1}{h_{c,o}\left(\frac{A_{p,o}}{A_o} + \frac{A_f \eta_{f,dry}}{A_o}\right)} \tag{21}$$

The corresponding dry fin efficiency $\eta_{f,dry}$ adopts Schmidt's approximation [19]:

$$\eta_{f,dry} = \frac{\tanh M_M r_i \theta}{M_M r_i \theta} \tag{22}$$

where

$$M_M = \sqrt{\frac{2h_{c,o}}{k_f t}} \tag{23}$$

Hong and Webb [20] slightly modified Eq. (22) to increase its approximation accuracy in the following form:

$$\eta_{f,dry} = \frac{\tanh(M_M r_i \theta)\cos(0.1 M_M r_i \theta)}{M_M r_i \theta} \tag{24}$$

Kern and Kraus [25] presented the analytical formulation for the circular fin.

$$\eta_{f,dry} = \frac{2r_i}{M_M(r_o^2 - r_i^2)}\left[\frac{K_1(M_M r_i)I_1(M_M r_o) - K_1(M_M r_o)I_1(M_M r_i)}{K_1(M_M r_o)I_0(M_M r_i) + K_0(M_M r_i)I_1(M_M r_o)}\right] \tag{25}$$

The procedure for WDFM can be found in Pirompugd et al. [23,24]. For further analyzing the surface condition along a real heat exchanger, the surface condition does not always complied with either fully dry or fully wet. Instead, the partially wet surface condition may occur in the tiny segments as shown in Fig. 6 in which the corresponding dew point temperature of moist air is between the outside tube temperature and the fin tip temperature. To tackle this difficulty, Pirompugd et al. [26,27] present a new method called the "finite circular fin method (FCFM)"

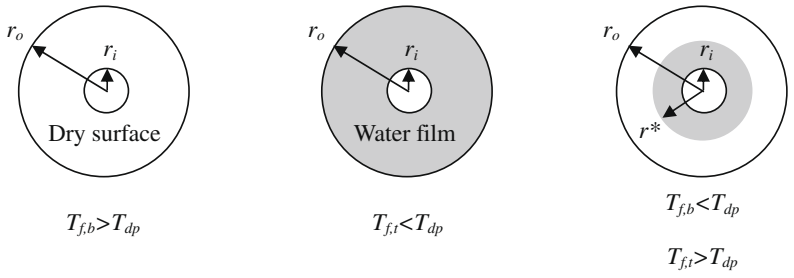

(6.1) Fully dry condition (6.2) Fully wet condition (6.3) Partially wet condition

Fig. 6. Circular fin in fully dry, fully wet and partially wet surface conditions.

which not only keep all the features in TTM and WDFM. For the FCFM but also can handle the fully wet, fully dry, and partially wet surface conditions as shown in Fig. 6. The details for FCFM can be found in Pirompugd et al. [26,27]. For the partially wet surface condition, the rate equations Eqs. (1)–(8) still holds but with the need to adjust the corresponding fin efficiency. Pirompugd et al. [26,27] proposed the fin efficiency for the circular fin under partially wet surface condition based on the enthalpy difference.

$$\eta_{f,part} = \frac{2r_i}{M_T(r^{*2} - r_i^2)\theta_{wet,r_i} + M_T C_{p,a}\theta_{dry,r^*}(r_o^2 - r^{*2})} \times \left[\frac{\beta K_1(M_T r_i) - \alpha I_1(M_T r_i)}{M_T I_1(M_T r^*)K_0(M_T r_i) + M_T I_0(M_T r_i)K_1(M_T r^*)}\right], \quad (26)$$

where

$$\alpha = \theta_{wet,r_i} M_T K_1(M_T r^*) + \gamma K_0(M_T r_i), \quad (27)$$

$$\beta = \theta_{wet,r_i} M_T I_1(M_T r^*) - \gamma I_0(M_T r_i), \quad (28)$$

$$\gamma = b'_{w,f}\theta_{dry,r^*} M_M \left[\frac{K_1(M_M r_o)I_1(M_M r^*) - I_1(M_M r_o)K_1(M_M r^*)}{K_1(M_M r_o)I_0(M_M r^*) + I_1(M_M r_o)K_0(M_M r^*)}\right]. \quad (29)$$

However, the partially wet fin efficiency in Eq. (26) can not be directly applied to Eq. (5) due to different driving potentials in fully dry (temperature) and fully wet (enthalpy) conditions. Hence it is modified to take into account both potentials for the partially wet condition. In this regard, the overall heat transfer coefficient (Eq. (5)) can be calculated by substitution of the effective wet fin efficiency, yielding:

$$\eta'_{f,part} = \frac{\dot{Q}_{wet,conv,\max} + \dot{Q}_{dry,conv,\max}}{\dot{Q}'_{wet,conv,\max}}\eta_{f,part}. \quad (30)$$

There are a number of publication concerning the partially wet fin efficiency for straight fin and circular fin, or even extension the straight fin to the circular fin. For example, Rosario and Rahman [28] presented the partially wet fin efficiency for circular fin as

$$\eta_{f,part} = \left(\frac{r^{*2}}{r_o^2}\right)\eta_{f,dry} + \left(1 - \frac{r^{*2}}{r_o^2}\right)\eta_{f,wet}. \quad (31)$$

Nevertheless, those fin efficiency can not directly fit into the heat transfer equation based on the enthalpy potential. This is because that calculation of the partially wet fin efficiency involves fully dry and fully wet portions. The former involves only sensible heat transfer obtained from temperature difference whereas the latter includes both sensible and latent heat transfer termed as enthalpy difference. Thus it can not be applied based on the enthalpy difference alone.

3.2. Equivalent dry-bulb temperature method

Wang and Hihara [29] presented a new method namely "equivalent dry-bulb temperature method (EDT)". With the definition of EDT method, the enthalpy difference is replaced by the equivalent dry-bulb temperature difference, yielding

$$\dot{Q}_{wet} = U_{o,d}A_o(T_a^e - T_r)F \quad (32)$$

The overall heat transfer coefficient, $U_{o,d}$ is the same as that of Eq. (21) but the dry fin efficiency must be substituted by the wet fin efficiency. The variable of T_a^e is the equivalent dry-bulb temperature that obtained from the constant enthalpy line in the psychrometric chart. Wang and Hihara [29], Xia and Jacobi [30] and Huzayyin et al. [31] show that Eq. (32) is capable of handling partially wet surface condition by modifications to the equivalent dry-bulb temperature and fin efficiency. The details for derivation of T_a^e for the fully wet and partially wet surface conditions can be found in the published literature. However, for the partially wet condition, a combination of either the FCFM with the EDT method gives the better simulation.

4. Mathematical model for mass transfer

The cooling and dehumidifying of moist air by a cold surface involves simultaneously heat and mass transfer. Therlkeld [4] described the process line equation:

$$\frac{di_a}{dW_a} = R\frac{(i_a - i_{s,p,o})}{(W_a - W_{s,p,o})} + (i_g - 2501R), \quad (33)$$

where R represents the ratio of sensible heat transfer characteristics to the mass transfer performance.

$$R = \frac{h_{c,o}}{h_{d,o}C_{p,a}}. \quad (34)$$

For easier manipulation, many researches simply presume the ratio is a constant value (≈1). Hence, one can easily obtain the mass transfer coefficient from Eq. (34). However, it should be made clear that the original heat-mass transfer analogy is valid only when the temperature and concentration fields are independent with each other. During the dehumidifying process, the temperature gradient is directly responsible for establishing the concentration gradient. Thus, these fields are not truly independent. This is especially applicable for turbulent flow conditions where the concentration boundary layer thickness is not independent of the temperature boundary layer thickness. As a result, the heat-mass transfer analogy is not expected to hold. For heat and mass transfer at the interface, the following equations hold:

$$h_{c,o}\Delta T = -k\left.\frac{dT}{dy}\right|_i \quad (35)$$

$$k_m\Delta c = -D\left.\frac{dc}{dy}\right|_i \quad (36)$$

In the foregoing equations, ΔT and Δc are the temperature difference and concentration difference between the ambient and the interface, respectively. The subscript i denotes at the water/vapor interface. Adopting the definitions of Nusselt number and Sherwood number, i.e. Nu = hL/k and Sh = k_mL/D (L represents certain characteristics length), one can arrive the following equations from Eqs. (35) and (36):

$$Nu = \frac{L}{\Delta T}\left(-\left.\frac{dT}{dy}\right|_i\right), \quad (37)$$

$$Sh = \frac{L}{\Delta c}\left(-\left.\frac{dc}{dy}\right|_i\right). \quad (38)$$

Dividing Eq. (37) with Eq. (38) yields:

$$\frac{Nu}{Sh} = \left(\frac{-\left.\frac{dT}{dy}\right|_i}{-\left.\frac{dc}{dy}\right|_i}\right)\frac{\Delta c}{\Delta T} \quad (39)$$

For the case of independent heat and mass transfer, the temperature gradient and concentration gradient do not interact with each other, the above equation is often correlated in the famous form as

$$\frac{Nu}{Sh} = \left(\frac{r}{Sc}\right)^{1/3}. \quad (40)$$

For dehumidification process, the interface concentration is regarded as saturated and is related to the interface temperature. Hence $c_i = c_i(T)$, Eq. (39) can be rewritten as

$$\frac{Nu}{Sh} = \left(\frac{dT}{dc}\right)\Big|_i \frac{\Delta c}{\Delta T} = \frac{\frac{\Delta c}{\Delta T}}{\left(\frac{dc}{dT}\right)\Big|_i}. \quad (41)$$

Based on the derived Eq. (41), let's consider a general case of dehumidification from the psychrometric chart. Note that the humidity ratio W is usually used as the driving potential of mass transfer for dehumidification instead of concentration. The shape of the relation curve from psychrometric chart for the humidity vs. temperature is "concave upwards". Thus the interfacial temperature rises when the inlet frontal velocity is increased. This is applicable even when the tube side temperature is fixed (evaporation inside tube) due to increased heat transfer rate with the rise of frontal velocity. As a consequence, one can see the value of $\left(\frac{dc}{dT}\right)\big|_i$ increases when the frontal velocity is increased. In the meantime, the value of $\frac{\Delta c}{\Delta T}$ is also increased. However, one can easily find out that the increasing rate of $\left(\frac{dc}{dT}\right)\big|_i$ slightly exceeds that of $\frac{\Delta c}{\Delta T}$. This suggests the difference between denominator and numerator of Eq. (41) is being increased when the frontal velocity is increased, thereby showing a variable ratio of $h_{c,o}/h_{d,o}C_{p,a}$ during dehumidification.

The foregoing discussion suggests that the ratio R depends on the air flow conditions and should not be regarded as a constant. In addition, Eq. (33) did not correctly describe the dehumidification process on the psychrometric chart. This is because the saturated air enthalpy at the mean temperature at the fin surface is different from that at the fin base. Pirompugd et al. [21,22] presented the new process line equation for TTM.

$$\frac{di_a}{dW_a} = \frac{R\cdot(i_{a,m}-i_{s,p,o,m}) + R\cdot(\varepsilon-1)\cdot(i_{a,m}-i_{s,w,f,m})}{(W_{a,m}-W_{s,p,o,m}) + (\varepsilon-1)\cdot(W_{a,m}-W_{s,w,f,m})}, \tag{42}$$

where

$$\varepsilon = \frac{A_o}{A_{p,o}}. \tag{43}$$

The process line equation (Eq. (42)) with TTM is applied by dividing the fin-and-tube heat exchanger into many tiny segments (Fig. 4) with all segments being fully wet surface condition. Pirompugd et al. [23,24] later on improved the model with this process line equation (Eq. (42)) and WDFM through which the divided segments are either fully wet or fully dry surface condition (Fig. 5). For a further general approach to the deal with the partial wet surface conditions, Pirompugd et al. [26,27] extended the model to FCFM that can take care of fully dry, fully wet, and partially wet conditions (Fig. 6). For all tiny segments under partially wet surface conditions (Fig. 6), Pirompugd et al. [26,27] proposed the new process line equation applicable to the circular fin under partially wet surface condition.

$$\frac{di_a}{dW_a} = \frac{R\cdot(i_{a,m}-i_{s,p,o,m}) + R\cdot\left(\frac{r^{*2}-r_i^2}{r_o^2-r_i^2}\right)\cdot(\varepsilon-1)\cdot(i_{a,m}-i_{s,w,f,m}) + R\cdot\left(\frac{r_o^2-r^{*2}}{r_o^2-r_i^2}\right)\cdot(\varepsilon-1)\cdot C_{p,a}(T_{a,m}-T_{f,m})}{(W_{a,m}-W_{s,p,o,m}) + \left(\frac{r^{*2}-r_i^2}{r_o^2-r_i^2}\right)\cdot(\varepsilon-1)\cdot(W_{a,m}-W_{s,w,f,m})} \tag{44}$$

From the FCFM and the new process line equations (Eqs. (42), (44)), the percent of wet surface of fin-and-tube heat exchanger can be identified, leading to higher predictive accuracy of the model.

5. Results and discussion

From the published results, many authors showed that the heat transfer characteristic (in terms of Colburn *j-factor)* is virtually independent on the fin spacing especially for heat exchangers having larger number of tube row and operated under fully dry surface condition. For example, when operated at the fully dry condition and $N \geqslant 4$, Wang et al. [32] and Rich [33] showed that the heat transfer characteristic is insensitive to the fin spacing. However, for $N = 1$ and 2, Wang and Chi [34] reported that the heat transfer characteristic decreases with the increase of fin spacing. This is especially pronounced when $Re_{Dc} < 5000$ and is confirmed with the published literature of Saboya and Sparrow [35]. Their results indicated that the boundary development is the most crucial factor for the 1-row coil, yet the effect of flow inertia takes control at higher Reynolds number. Therefore, for fully dry surface, the effect of fin spacing diminished for $Re_{Dc} > 5000$. For $Re_{Dc} < 5000$, the heat transfer characteristic increases with decrease of fin spacing. This phenomenon is seen for $N \leqslant 2$, and is especially pronounced for $N = 1$. By contrast for heat exchangers being tested under dehumidification, the corresponding sensible heat transfer performance exhibits a comparatively insensitive influence to the change of fin spacing for $N = 1$ and $N = 2$. Apparently, the results are attributed to the presence of condensate under dehumidification. This appearance of condensate plays a role to alter the airflow pattern, roughening the fin surface and providing a better mixing of the airflow. As a consequence, the influence of fin pitch is reduced accordingly. This phenomenon is analogous to using the enhanced fin surface in fully dry condition. For enhanced surfaces such as slit and louver fin geometry, Du and Wang [36] and Wang et al. [37,38] reported a negligible effect of fin spacing even for $N = 1$ or $N = 2$. Moreover, based on the numerical simulation by Torikoshi et al. [39], they found that the vortex forming behind the tube can be suppressed and the entire flow region can be kept steady and laminar when the fin spacing is small enough. A further increase of fin spacing would result in a noticeable increase of cross-stream width of the vortex region behind the tube. As a result, the heat transfer characteristic decreases with the increase of fin spacing for the one-row configuration, indicating a detectable influence of fin spacing. For fully wet surface, the presence of condensate that provides a good air flow mixing even at larger fin spacing. In fact, the heat transfer characteristic slightly decreases with the increase of number of tube row. However, the difference in the heat transfer characteristic becomes even more negligible when the number of tube rows is increased. With the increase in the number of tube rows, the condensate blow-off phenomenon from the preceding row is blocked by the subsequent row.

From the process line equation, Pirompugd et al. [21,22] show about 20–40% increase of mass transfer characteristic when the inlet relative humidity is increased from 50% to 90%. However, for the TTM, Pirompugd et al. [21,22] show relatively small influence of the inlet relative humidity. Hence, it is expected that the associated influence on the mass transfer characteristic is also small. Pirompugd et al. [23,24,26,27] show a detectable rise of the increase of mass transfer characteristic when the inlet relative humidity is decreased at high Re_{Dc}. The phenomenon is actually in line with the basic derivation of Eq. (41). With the original procedures of Threlkeld method, it was only applicable to the counter-cross flow arrangement and it also excludes the influence of primary surface. Hence the TTM is more appropriate than the original procedures of Threlkeld method in reducing the mass transfer coefficient under fully wet conditions. Moreover, the WDFM and FCFM are more appropriate than Threlkeld's method or TTM for the fully and partially wet conditions. For the rising mass transfer characteristic at high Re_{Dc} and its decreasing performance with the inlet relative humidity, it is in connection with the blow-off of condensate at larger Re_{Dc} which make more room for water vapor to condensate along the surface

and even results in the partially dry condition due to the rise of dew point temperature. This phenomenon becomes less pronounced with the rise of the number of tube row for condensate blow-off may be blocked by the subsequent tube row.

For the friction factor, Wang et al. [6,9] presented that their experimental data indicate a significant increase of friction factor under dehumidifying condition. In fact, the friction factor is approximately 60–120% higher than those of the dry condition. In addition, the friction factors are insensitive to the change of relative humidity.

6. Conclusion

The present study provides a survey about the data reduction methods for fin-and-tube heat exchangers being operated at dehumidification where both heat and mass transfer must be taken into account simultaneously. The data reduction methods includes the original Threlkeld method, direct method, the equivalent dry-bulb method, tube by tube method, the fully wet and fully dry tiny circular fin method, and the finite circular fin method. Based on the foregoing discussion, the following results are concluded.

1. Threlkeld method, the direct method (enthalpy potential and temperature difference method) and the equivalent dry-bulb temperature method (EDT method) is based on the original lump method are the basic reduction method for reducing the results. However, they are unable to predict the partially wet surface.
2. The tube-by-tube method (TTM) stems from the Threlkeld method and is able to account for the influence of temperature variation in both tube and air-side. However, it can not predict the partially wet surface.
3. The fully wet and fully dry tiny circular fin method (WDFM) developed from TTM can divide the fin-and-tube heat exchangers into many tiny segments through which one can identify the surface conditions to be either fully dry or fully wet condition. The proposed method can handle both cases with either fully dry or fully wet but is unable to deal with the tiny surface where both dry/wet conditions prevail.
4. By proposing the partially wet fin efficiency, the proposed the finite circular fin method (FCFM) resolve all the surface conditions, fully dry, fully wet, and even partially wet condition occurring in the tiny element.
5. The mass transfer characteristics can be obtained from the modified process line equation incorporated with the preceding methods (WDFM or FCFM). The conventional assumption of constant ratio ($h_{c,o}/h_{d,o}C_{p,a} \approx$ constant) is actually incorrect.

Acknowledgements

The authors are indebted to the Thailand Research Fund (TRF) and Commission on Higher Education of Thailand (CHE) and Support Fund for Research and Development (No. 40/2550) from Faculty of Engineering, Burapha University and the Energy R&D foundation funding from the Bureau of Energy of the Ministry of Economic Affairs, Taiwan for supporting this study.

References

[1] ASHRAE Standard 41.2-1987. Standard methods for laboratory air-flow measurement. American Society of Heating, Refrigerating and Air-Conditioning Engineers, Inc., Atlanta, GA, 1987.
[2] ASHRAE Standard 41.1-1986, Standard method for temperature measurement. American Society of Heating, Refrigerating and Air-Conditioning Engineers, Inc., Atlanta, GA, 1986.
[3] ASHRAE Standard 33-2000, Method of testing forced circulation air cooling and air heating coils. American Society of Heating, Refrigerating and Air-Conditioning Engineers, Inc., Atlanta, GA, 2000, pp. 33–78.
[4] J.L. Threlkeld, Thermal Environmental Engineering, Prentice-Hall, Inc., New York, NY, 1970.
[5] A.M. Jacobi, V.W. Goldschmildt, Low Reynolds number heat and mass transfer measurements of an overall counter-flow baffled finned-tube condensing heat exchanger, J. Heat Transf. 33 (4) (1990) 755–765.
[6] C.C. Wang, Y.C. Hsieh, Y.T. Lin, Performance of plate finned tube heat exchangers under dehumidifying conditions, J. Heat Transf. 119 (1997) 109–117.
[7] J.M. Corberan, M.G. Melon, Modelling of plate finned tube evaporators and condensers working with R134a, Int. J. Refrig. 21 (4) (1998) 273–284.
[8] C.C. Wang, Y.T. Lin, C.J. Lee, An airside correlation for plain fin-and-tube heat exchangers in wet conditions, Int. J. Heat Mass Transf. 43 (2000) 1869–1872.
[9] C.C. Wang, Y.T. Lin, C.J. Lee, Heat and momentum transfer for compact louvered fin-and-tube heat exchangers in wet conditions, Int. J. Heat Mass Transf. 43 (2000) 3443–3452.
[10] M.H. Kim, C.W. Bullard, Air-side performance of brazed aluminum heat exchangers under dehumidifying conditions, Int. J. Refrig. 25 (7) (2002) 924–934.
[11] C.C. Wang, W.S. Lee, W.J. Sheu, Y.J. Chang, A comparison of the airside performance of the fin-and-tube heat exchangers in wet conditions; with and without hydrophilic coating, Appl. Therm. Eng. 22 (2002) 267–278.
[12] M.H. Kim, S. Song, C.W. Bullard, Effect of inlet humidity condition on the air-side performance of an inclined brazed aluminum evaporator, Int. J. Refrig. 25 (2002) 611–620.
[13] M.H. Kim, S.Y. Lee, S.S. Mehendale, R.L. Webb, Microchannel heat exchanger design for evaporator and condenser applications, Adv. Heat Transf. 37 (2003) 297–429.
[14] T.R. Bump, Average temperatures in simple heat exchangers, J. Heat Transf. 85 (2) (1963) 182–183.
[15] R.J. Myers, The effect of dehumidification on the air-side heat transfer coefficient for a finned-tube coil, MS Thesis, University of Minnesota, Minneapolis, 1967.
[16] V. Gnielinski, New equation for heat and mass transfer in turbulent pipe and channel flow, Int. Chem. Eng. 16 (1976) 359–368.
[17] F.C. McQuiston, Fin efficiency with combined heat and mass transfer, ASHRAE Transactions Part 1 81 (1975) 350–355.
[18] F.C. McQuiston, J.D. Parker, Heating Ventilating and Air Conditioning, 4th ed., John Wiley & Sons Inc., New York, NY, 1994. p. 594.
[19] Th.E. Schmidt, Heat transfer calculations for extended surfaces, Ref. Eng. 49 (1949) 351–357.
[20] T.K. Hong, R.L. Webb, Calculation of fin efficiency for wet and dry fins, Int. J. HVAC&R Res. 2 (1) (1996) 27–41.
[21] W. Pirompugd, S. Wongwises, C.C. Wang, A tube-by-tube reduction method for simultaneous heat and mass transfer characteristics for plain fin-and-tube heat exchangers in dehumidifying conditions, Heat Mass Transf. 41 (8) (2005) 756–765.
[22] W. Pirompugd, S. Wongwises, C.C. Wang, Simultaneous heat and mass transfer characteristics for wavy fin-and-tube heat exchangers under dehumidifying conditions, Int. J. Heat Mass Transf. 49 (1–2) (2006) 132–143.
[23] W. Pirompugd, W.C.C. Wang, S. Wongwises, A fully wet and fully dry tiny circular fin method for heat and mass transfer characteristics for plain fin-and-tube heat exchangers under dehumidifying conditions, J. Heat Transf. 129 (9) (2007) 1256–1267.
[24] W. Pirompugd, W.C.C. Wang, S. Wongwises, Heat and mass transfer characteristics for finned tube heat exchangers with humidification, J. Thermophys. Heat Transf. 21 (2) (2007) 361–371.
[25] D.Q. Kern, A.D. Kraus, Extended Surface Heat Transfer, McGraw-Hill Inc., New York, NY, 1972. pp. 88–106.
[26] W. Pirompugd, C.C. Wang, S. Wongwises, Finite circular fin method for heat and mass transfer characteristics for plain fin-and-tube heat exchangers under fully and partially wet surface conditions, Int. J. Heat Mass Transf. 50 (3–4) (2007) 552–565.
[27] W. Pirompugd, C.C. Wang, S. Wongwises, Finite circular fin method for wavy fin-and-tube heat exchangers under fully and partially wet surface conditions, Int. J. Heat Mass Transf. 51 (15–16) (2008) 4002–4017.
[28] L. Rosario, M.M. Rahman, Analysis of heat transfer in a partially wet radial fin assembly during dehumidification, Int. J. Heat Fluid Fl. 20 (1999) 642–648.
[29] J. Wang, E. Hihara, Prediction of air coil performance under partially wet and totally wet cooling conditions using equivalent dry-bulb temperature method, Int. J. Refrig. 26 (2003) 293–301.
[30] Y. Xia, A.M. Jacobi, Air-side data interpretation and performance analysis for heat exchangers with simultaneous heat and mass transfer: wet and frosted surfaces, Int. J. Heat Mass Transf. 48 (2005) 5089–50102.
[31] A.S. Huzzayyin, S.A. Nada, H.F. Elattar, Air-side performance of wavy-finned-tube direct expansion cooling and dehumidifying air coil, Int. J. Refrig. 30 (2) (2007) 230–244.
[32] C.C. Wang, Y.C. Hsieh, Y.J. Chang, Y.T. Lin, Sensible heat and friction characteristics of plate fin-and-tube heat exchangers having plane fins, Int. J. Refrig. 19 (4) (1996) 223–230.
[33] D.G. Rich, The effect of fin spacing on the heat transfer and friction performance of multi-row, plate fin-and-tube heat exchangers, ASHRAE Transactions 79 (2) (1973) 137–145.

[34] C.C. Wang, K.U. Chi, Heat transfer and friction characteristics of plain fin-and-tube heat exchangers: Part I: new experimental data, Int. J. Heat Mass Transf. 43 (2000) 2681–2691.
[35] F.E.M. Saboya, E.M. Sparrow, Transfer characteristics of two-row plate fin and tube heat exchanger configuration, Int. J. Heat Mass Transf. 19 (1) (1976) 41–49.
[36] Y.J. Du, C.C. Wang, An experimental study of the airside performance of the superslit fin-and-tube heat exchangers, Int. J. Heat Mass Transf. 43 (2000) 4475–4482.
[37] C.C. Wang, Y.J. Chang, K.U. Chi, Y.P. Chang, An experimental study of heat transfer and friction characteristics of typical louver fin-and-tube heat exchangers, Int. J. Heat Mass Transf. 41 (1998) 817–822.
[38] C.C. Wang, C.J. Lee, C.T. Chang, S.P. Lin, Heat transfer and friction correlation for compact louvered fin-and-tube heat exchangers, Int. J. Heat Mass Transf. 42 (1999) 1945–1956.
[39] K. Torikoshi, G. Xi, Y. Nakazawa, H. Asano, Flow and heat transfer performance of a plate-fin and tube heat exchanger (1st report: effect of fin pitch), in: 10th International Heat Transfer Conference 1994 paper 9-HE-16, 1994, pp. 411–416.